Journal of Cleaner Production 179 (2018) 42–54

Contents lists available at ScienceDirect

Journal of Cleaner Production

journal homepage: www.elsevier.com/locate/jclepro

Synthesis and characterizations of a novel FeNi3/SiO2/CuS magnetic nanocomposite for photocatalytic degradation of tetracycline in simulated wastewater

Negin Nasseh [a], Lobat Taghavi [a], Behnam Barikbin [b, *], Mohammad Ali Nasseri [c]

[a] Department of Environmental Science, Faculty of Natural Resources and Environment, Science and Research Branch, Islamic Azad University, Tehran, Iran
[b] Social Determinants of Health Research Center, Environmental Health Engineering Department, Health School Birjand University of Medical Sciences, Birjand, Iran
[c] Department of Chemistry, Faculty of Science, University of Birjand, Birjand, Iran

ARTICLE INFO

Article history:
Received 7 October 2017
Received in revised form
2 January 2018
Accepted 4 January 2018
Available online 10 January 2018

Keywords:
$FeNi_3/SiO_2/CuS$
Photocatalyst
UV light
Tetracycline
Aqueous solutions
Kinetic

ABSTRACT

In recent decades, application of magnetic nanocomposites as a catalyst to remove organic contaminants and antibiotics has attracted a great deal of attention on account of having production simplicity, stability and recyclability, operating under environmental conditions, high chemical stability and easier separation, as well as full degradability of organic materials. This experimental research was conducted at laboratory scale with the aim of investigating the efficiency of a new magnetic nanocatalyst ($FeNi_3/SiO_2/CuS$) for degradation of tetracycline-the second common group of antibiotics in terms of production and consumption in the world-in the presence of ultraviolet light in aqueous solutions. To this end, first, $FeNi_3/SiO_2/CuS$ was synthesized. The morphology and other characteristics of the produced nanocatalyst were specified by X-ray diffraction, energy dispersive spectroscopy, field emission scanning electron microscopy, vibration sampling magnetometer, and transmission electron microscopy. The factors influencing tetracycline removal by the mentioned nanophotocatalyst, including pH (3, 5, 7, 9), contact time (5–200 min), contaminant concentration (10–30 mg L^{-1}), and nanocomposite dose (0.005 –0.1 g L^{-1}), were studied. The results indicated that $FeNi_3/SiO_2/CuS$ possess accumulation and agglomeration structure, good monodispersity, superior magnetic properties (Ms = 19.42 emu g^{-1}). In addition, the findings showed that with elevation of pH, the percentage of degradation increased from 75.6 to 99.5%, and when the nanocatalyst dose and the initial concentration of the contaminant reduced, the removal percentage increased (95.54–57.7%) and (96.71–78.21%), respectively, so that under optimal conditions (tetracycline concentration: 10 mg L^{-1}, time: 200 min, pH = 9, nanocatalyst dose: 0.005 g L^{-1}), the efficiency of the photocatalytic process using $FeNi_3/SiO_2/CuS$ in tetracycline degradation reached almost 100% and the mineralization rate was 64.96%. Furthermore, the kinetics of the rate of this pollutant degradation followed pseudo-first-order kinetics ($R^2 > 0.98$) and the constant rate of degradation was obtained as 0.0257 min^{-1}. The findings suggested that after five cycles, the nanocatalyst efficiency did not decrease significantly, such that the removal efficiency showed a reduction of only 15% from the first to the last cycle. Eventually, based on the results obtained in the present study, it can be concluded that the $FeNi_3/SiO_2/CuS$ photocatalytic process enjoys a suitable efficiency for the removal of tetracycline from aqueous solutions.

1. Introduction

Nowadays, a growing public concern has been aroused over the issue of environmental pollution (Song et al., 2017). Antibiotics are man-made organic materials traditionally used for preventing human and animal infections. These materials are considered as emerging pollutants and today, include a major part of research related to water and wastewater treatment (Lu et al., 2013). Annual consumption of antibiotics in the world has been estimated to be between 100,000 and 200,000 tons. Following consumption,

* Corresponding author.
E-mail address: Barikbin@bums.ac.ir (B. Barikbin).

https://doi.org/10.1016/j.jclepro.2018.01.052
0959-6526/

antibiotics are seldom metabolized completely in the body, so that 30–90% of them remain active after discharge (Wang et al., 2017). Accordingly, it can be concluded that annually in good conditions 30,000 but in bad conditions 180,000 tons of active antibiotics enter into the environment. Indeed, these chemical compounds can cause contamination of natural environment by developing biological imbalance and bacterial resistance (Almasi et al., 2016). Tetracycline [TC] is a bacteriostatic antibiotic that affects gram-positive and gram-negative bacteria as well as some mycoplasmas and fungi. TC is used for the selective treatment of infections resulting from chlamydia (cause of trachoma disease, salpingitis, urethritis, and lymphogranuloma venereum), Rickettsia (cause of Q fever disease) and mycoplasma. Regarding its mechanism of action, TC develops disorder in the protein-making of bacteria (by affecting bacterial ribosomes) and prevents their growth and proliferation (Daghrir and Drogui, 2013). Moreover, TC has damaging effects on microbial respiration, nitrification process, and regeneration of iron (III) in soil. Therefore, due to high consumption of antibiotics, their concentration in water increases, resulting in diminished water quality (Katipoglu- yazan et al., 2015). The physiochemical property of tetracycline is summarized in Table 1(Oturan et al., 2013). Moreover, Fig. 1 shows the chemical structure and functional groups of TC in different pHs in aqueous solution. Thus far, various methods have been used for the removal of residuals of TC from aqueous environments. Studies have shown that absorption methods with the help of activated carbon (Saygılı and Guzel, 2016), ion exchange (Ma et al., 2014), membrane processes (Liu et al., 2016), Chemical Coagulation Method (Saitoh et al., 2017) and materials such as montmorillonite (Papolo et al., 2008), aluminum oxide [Al_2O_3] (Chen and Huang, 2010), chitosan (Caroni et al., 2009) can be effective in removal of TC. These methods are often ineffective at low concentrations and are non-economical. For instance, in the adsorption process, the contaminant is adsorbed by the adsorbent and no change is developed in its structure, and it only changes from solution phase to solid phase. On the other hand, some adsorbents such as activated carbon are costly and not economical (Amouzgar and Salamatinia, 2015). The membrane processes are not economical due to high cost of investment, operation and maintenance. The chemical coagulation method requires chemicals and produces large amount of sludge during the process (Saitoh et al., 2017). The disadvantages of the ion exchange method include consumption of large amounts of chemicals for regeneration and occupation of larger space considering the volume of water produced (Salvestrin and Hagare, 2009). Therefore, based on the results of various studies, it can generally be concluded that the elimination of antibiotics by physical methods does not have sufficient efficiency, also biological and chemical treatments are associated with long-term problems for the first one and the production of harmful side-effects for the latter. Therefore, it is evident that the prospect of developing more efficient and durable systems has become necessary (Assadi et al., 2012). Advanced oxidation processes [AOP_S] are the most effective and efficient technologies for the decomposition and elimination of dangerous, biocompatible, and non-degradable organic pollutants in aquatic environments, which have been widely utilized over the past decades, and have played an important role in water and wastewater treatment. The main mechanism of these processes is based on the production of hydroxyl radicals, which are almost able to oxidize most of the organic compounds quickly but non-selectively (Safari et al., 2015). Different advanced oxidation processes such as ozonation (Wang et al., 2011), Fenton or electro Fenton (Barhoumi et al., 2017), ultraviolet radiation (Safari et al., 2015), etc. have been used to remove organic pollutants, especially antibiotics from water. Among the various processes of advanced oxidation, photocatalysis, as a friendly environmental treatment process is one of the most innovative and promising technologies that has been considered in recent years to eliminate organic pollutants and microbial agents due to its low

Table 1
The chemical specifications of the tetracycline used in this research.

Tetracycline	Chemical formula	Molecular weight (g mol^{-1})	Solubility (mol l^{-1})	pKa_1	pKa_2	pKa_3
TC	$C_{22}H_{24}N_2O_8$.HCL	480.9	0.041	3.2 ± 0.3	7.78 ± 0.05	9.6 ± 0.3

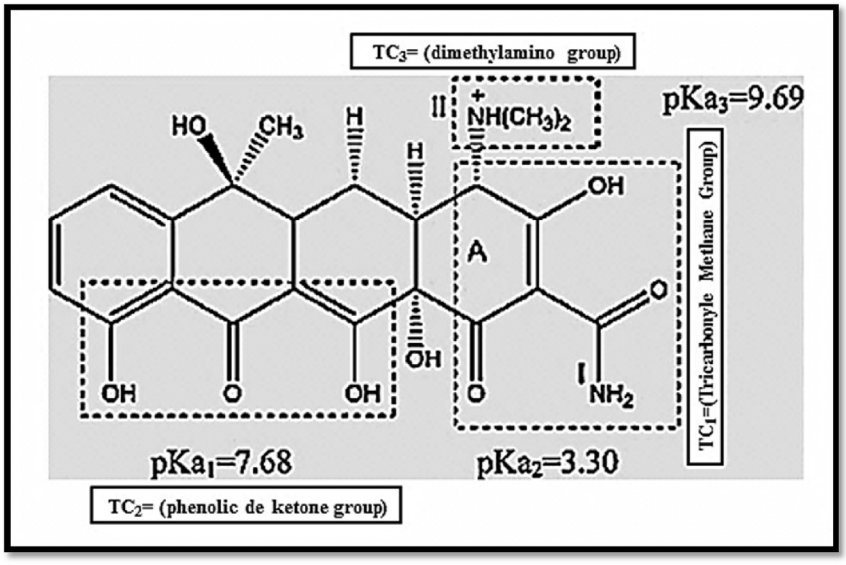

Fig. 1. Chemical structure and chart of TC species in aqueous solutions.

environmental problems. Semiconductor photocatalyst technology, as a new eco-friendly technology, has many advantages in contributing to the degradation of pollutants, such as: excessive activity of optical degradation and not producing the secondary pollution. At the same time, some specific semiconductor photocatalyst are non-toxic, stable and recyclable, cheap, etc. Therefore, the technology of semiconductor photocatalyst is used in anti-corrosion, air purification, antibacterial, fields as well as water quality improvement. Besides, this technology has many enormous economic and social benefits. Many semiconductors such as tungsten trioxide [WO_3] (Singh et al., 2016), cadmium sulfide [CdS] (Vázquez et al., 2016), zinc oxide [ZnO] (Guo et al., 2014) and titanium oxide [TiO_2](Safari et al., 2015) have been studied as a catalyst, for the photocatalytic degradation of antibiotics. Among these photocatalysts, WO_3 is less available; cadmium itself is a toxic heavy metal and CdS is prone to easy deactivation and photo-corrosion (Assadi et al., 2012). ZnO and TiO_2 have wide bandgap; so, they can be activated in UV light area which is a little share of sunlight. Accordingly, these semiconductor photocatalysis have low efficiency in visible light (Johar et al., 2015). One of the important semiconductor materials which have excellent physical, chemical, electrical, magnetic as well as other properties is Copper sulfide [CuS] with a 2.0 eV band gap (Yang et al., 2014). In recent years, materials with organic-metal bond such as CuS have attracted a great deal of attention due to their high photocatalytic potential in the presence of UV radiation for removing organic compounds from aqueous environments. The most important advantage of such materials is the capability of absorbing a wide range of electromagnetic waves and their high efficiency in photocatalytic degradation of organic compounds. In addition, non-toxic, absence of limitation of mass transfer, operating under environmental conditions, high chemical stability within a wide range of pH, and great resistance to chemical breakdown and optical corrosion and so on are other major advantages of this catalytic process (Safari et al., 2015). Although these surfaces enhance the catalyzer's efficiency, the problem of their recyclability and reusability has not still been solved completely; therefore, traditional methods of filtration and centrifugation should still be used. On the other hand, due to entrapment of reactant materials and products in the pores of these preservatives, following several times of usage, their catalytic activity diminishes. To solve this problem, application of catalyzer systems based on magnetic nanoparticles has attracted attention, as magnetic nanoparticles provide reactive molecules with a large surface area and are also easily separable and reusable using an external magnet, after completion of the reaction. In recent decades, Nanotechnology has been a high potential for water and wastewater treatment (Song et al., 2016) and application of magnetic nanocomposites as catalysts for removal of organic contaminants and antibiotics. This has attracted a great deal of attention on account of their simple production and easier separation, as well as their full degradability of organic materials (Kakavandi et al., 2014).

$FeNi_3$ alloy is a magnetic material that is widely employed due to its high saturation magnetization, high permeability, high temperature and low energy losses. There are many concerns about the synthesis of $FeNi_3$ nanomaterials because each of these two metals has its own risk, especially nickel nanoparticles which may cause dermatitis and allergy, and in some cases may be carcinogenic. But fortunately, it has not yet been reported that $FeNi_3$ is harmful (Shekari et al., 2017). In spite of the large applications of magnetic particles in many cases and applied research, their intrinsic instability in their use over a long term is one of the major problems. Metal nanoparticles such as ($FeNi_3$) are chemically very active and are simply oxidized in the air and generally result in the loss of their magnetic properties and dispersion.

Therefore, keeping them stable for a long time without agglomerating or sedimentation is a very important issue. Stability is a decisive requirement for any application of magnetic nanoparticles. Especially for pure metals such as iron, nickel, cobalt and alloys that are very sensitive to air. It seems that a very simple method is protection with an impenetrable layer, so that oxygen cannot reach the surface of the magnetic particle (Nirpuel et al., 2014). All protective strategies result in magnetic nanoparticles with core-shell structure, so that the uncoated magnetic nanoparticle -the core-is isolated from the surrounding area by the shell. These grafting strategies involve coating with organic matter, including surface stabilizers or polymers, and coatings with mineral layers such as silica [SiO_2] or carbon. It is worthy of note that in many cases, the protective shells will also sustain the magnetic nanoparticles (Nasseri and Sadeghzadeh, 2013).

Accordingly, considering the disadvantages and adverse effects that antibiotic residuals may exert on the environment and since application of magnetic nanocomposites is an up-to-date research for water treatment, and also with regard to the high efficiency of oxidation processes in removing organic contaminants, the aim of this research was to investigate the photocatalytic efficiency of a new synthesized magnetic nanocomposite, $FeNi_3/SiO_2/CuS$ [FNSCS], in the presence of *ultraviolet light* [UV] for removing TC from aqueous environments.

2. Materials and methods

2.1. Materials

To synthesize FNSCS, polyethylene glycol (PEG) [$H(OCH_2CH_2)_nOH$] (1.0 g. MW 6000), bivalent iron chloride with the chemical formula of [$FeCl_2$ ($4H_2O$)], nickel chloride [$NiCl_2$ ($6H_2O$)], hydrated hydrazinium [$N_2H_4.H_2O$] with a purity percentage of 80%, tetra ethyl ortho silicate (TEOS) with the chemical formula of [$SiC_8H_{20}O_4$], copper sulfate [$CuSO_4$], ethylene glycol [$C_2H_6O_2$], and sodium thiosulfate [$Na_2S_2O_3$] were used, all of which were purchased from Merck Co. Germany, Furthermore, different concentrations of solutions containing the contaminant were prepared by dissolving TC hydrochloride salt [$C_{22}H_{24}O_8N_2.HCl$] (Sigma Aldrich), as provided in Table 1 with a purity of over 95%. Deionized water was used for preparation of solutions across all the stages.

2.2. The properties of the synthesized nanocomposite

Field emission scanning electron microscopy [FESEM] (SIGMA VP-500, Zeiss, Germany) was employed to study the shape, mean diameter, and details of the surface of FNSCS. Device X Pert Pro (Panalytical Co.) was used for X-ray diffraction [XRD] analysis in order to examine the composition and properties of the crystal structure of the nanocomposite. The average dimension (D) of nano particles was estimated by Debye–Sherrers Equation (Eslami et al., 2016).

$$D = \frac{0.98\lambda}{\beta\cos\theta} \quad (1)$$

In the above formula, D is the diameter of particles, β is the peak width of the diffraction peak profile at half maximum height resulting from small crystallite size (radians), θ is the diffraction angle at the site of peak, and λ is the X-ray wavelength of Cu K_α radiation (nm), ($\lambda = 0.1540$ nm).

In addition, transmission electron microscopy [TEM] device (EM10C-100 KV, Zeiss, Germany) was utilized to investigate the sample with a greater resolution and magnification. Quantitative detection of the constituent elements of the new synthesized

magnetic nanocomposite and their weight percentage were obtained by energy dispersive spectroscopy [EDS] (SIGMA VP-500, Zeiss, Germany). The magnetic rate of the synthesized magnetic nanoparticle was also determined using a vibration sampling magnetometer (VSM 7400).

2.3. Methods

2.3.1. Synthesis of $FeNi_3/SiO_2/CuS$ magnetic nanocomposite

First, based on previous studies, $FeNi_3/SiO_2$ was synthesized (Nasseri and Sadeghzadeh, 2013; Yang et al., 2015). Subsequently, 0.15 g of it was dispersed in 20 ml ethylene glycol (EG) for 30 min in an ultrasonic device. The dispersed materials were then poured into a 500 cc flask and placed inside oil bath at 120 °C. Thereafter, 0.8 g $CuSO_4$ was added to the above mentioned suspension and copper sulfate was completely dissolved into the contents inside the flask. Following this stage, 1.9 g $Na_2S_2O_3$, which had already been added to 20 ml EG, was poured into the suspension containing $FeNi_3/SiO_2$ and copper sulfate, and reflux operation of the sample was performed at 140 °C for 90 min. Following this time and once the flask cooled down, the obtained product was separated by N_{42} magnet and washed with ethanol once and with deionized water several times, and eventually dried at 80 °C in an oven for 5 h (Beyki et al., 2016). Some of the possible shortcomings of the synthesized photocatalyst are humidity, sensitivity and using vacuum conditions to prevent oxidation (Fe and Ni) (especially in the first stage of synthesis).

2.3.2. The experiments of adsorption and photocatalytic removal of TC

Stock solution (1000 mg L^{-1}) of dissolution of TC hydrochloride salt was prepared in deionized water. This solution was synthesized on a weekly basis and kept at 4 °C inside a refrigerator. The variables studied in this research were pH (3, 5, 7, 9), value of the magnetic nanocomposite (0.005, 0.01, 0.02, 0.03, 0.04, 0.05, and 0.1 g L^{-1}), initial concentration of TC (10, 15, 20, 25, 30 mg L^{-1}), and contact time (5, 10, 15, 30, 60, 90 and 200 min). A magnetic stirrer with 300 rpm was used for mixing the samples. In addition, to obtain pH_{zpc}, initial pH values of Sodium chloride [NaCl] solutions were adjusted to a value between 2 and 12 by adding 0.1 M *Hydrochloric acid* [HCl] or 0.1 M *sodium hydroxide* [NaOH] solutions. The FNSCS photocatalyst (0.1 g) was added to the solution and after 24 h shaking at 300 rpm; the pH_{final} was measured and plotted against $pH_{initial}$. The pH_{zpc} is the point where the curve crossed the line $pH_{initial} = pH_{final}$(Salarian et al., 2016). All the experiments were performed in a batch system at temperature (5–50 °C) on 200 ml samples (for adsorption experiments) and at room temperature (24 ± 2 °C) on 400 ml samples inside a 500 ml UV reactor (for photocatalytic process).

It should be mentioned that, in thepresent study, before performing the photocatalytic experiments of FNSCS in the presence of UV lamp, the container containing the contaminant and magnetic nanocomposite was exposed to darkness to perform sorption and desorption experiments for 30 min. Thereafter, its concentration was re-measured, which was obtained as almost 11 ± 2% and considered as the initial concentration of the photocatalytic process.

For radiation of UV, TUV PHILIPS PL-L with a nominal power of 18 W, wavelength of 254 nm and radiation intensity of 2500 mcW $(cm^2)^{-1}$ was used. This lamp was placed in the center of the reactor inside a quartz sheath. A cooling water wall was devised around the reactor, which was connected to the weak and direct stream of water and employed to keep the temperature of the sample inside the reactor within the range of 24 ± 2 °C. The samples were withdrawn from the reactor within certain time intervals using a sample withdrawal valve (Fig. 2). Following separation of the nanocomposite by the magnet, the residual concentration of TC was measured by a spectrophotometer device (UV/visible T80$^+$) at a wavelength of 358 nm (Liu et al., 2015).

Efficiency of the TC removal process was calculated according to Eq (2).

$$\text{Removal } \% = \left(1 - \frac{C_t}{C_0}\right) \times 100 \tag{2}$$

Where C_t and C_0 are the concentration of TC at the time of t and initial concentration of TC (mg L^{-1}), respectively, and R% represents the contaminant removal percentage.

Also the mineralization rate was calculated by using the formula (Lu et al., 2017b):

$$\text{Mineralization rate} = \left(1 - \frac{\text{organic carbon content after reaction}}{\text{total organic carbon content}}\right) \times 100 \tag{3}$$

2.3.3. Determination of kinetics of the reaction rate for degradation of TC

To examine the catalytic processes for wastewater treatment, especially pharmaceutical wastewaters, use of reaction rate kinetics is important. Based on studies, the pseudo-first-order [PFO] kinetics model is typically employed for describing photocatalytic degradation of different organic compounds, especially antibiotics (Safari et al., 2015).

In general, the rate of heterogeneous catalytic reactions is explained under the conditions of the Langmuir-Hinshelwood (L-H) kinetic model (Eslami et al., 2016).

$$r = k'\,\theta = -\frac{dc}{dt} = k'\left(\frac{kc}{1+kc}\right) \tag{4}$$

where r is the oxidation reaction rate ((mg L^{-1}) min^{-1}), K′ is equivalent to the reaction rate constant (min^{-1}), C is the

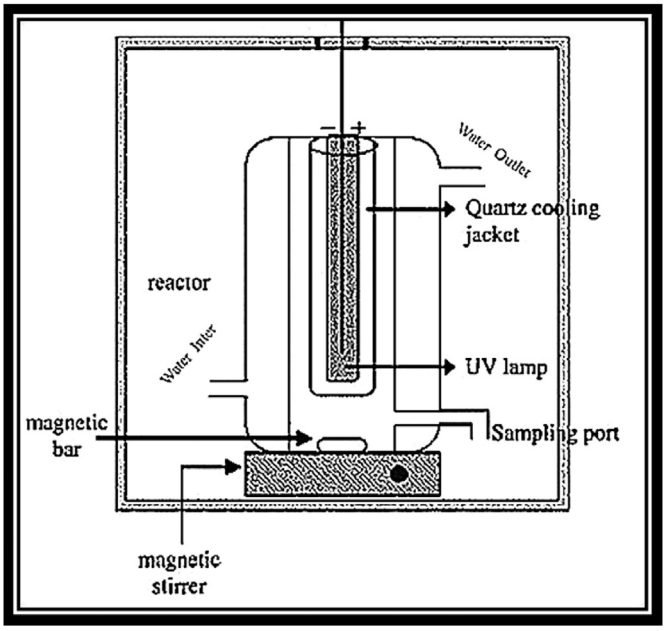

Fig. 2. Schematic drawing of the pilot UV used in study.

contaminant concentration (mg L^{-1}), K denotes the absorption coefficient of the reactant (mg^{-1}), and θ is the fractional site coverage for the reactant.

For solutions with a very low concentration (e.g., drugs in water) with K≪1, the L-H Equation (Equation (4)) is simplified into PFO kinetics:

$$\frac{dC}{dt} = k_{obs}C \quad (5)$$

$$\ln\left(\frac{C}{C_0}\right) = -k_{obs}t \quad (6)$$

In this equation, K_{obs} is the constant of the PFO reaction rate (min^{-1}), t denotes the reaction time (min), C is the residual concentration after the time of interest, and C_0 represents the initial concentration of the contaminant (mg L^{-1}).

3. Results and discussion

3.1. Characteristics of the synthesized nanocomposite

To investigate and confirm the accuracy of the magnetic nanoparticles in this study, morphological tests of TEM, SEM, EDX, VSM and XRD were performed.

3.2. $FeNi_3/SiO_2/CuS$

Fig. 3a shows the TEM image related to the nanocatalyst synthesized in this research with a magnification of 46,460 KX, suggesting that the images closer to the surface were images taken from the sample, the shape of the material did not change, suggesting amorphicity of this nanocomposite. Thus, no regular structure was suggested for it. Moreover, it can be clearly observed that the texture of the material in terms of agglomeration was highly agglomerated, suggesting high density of this material.

Furthermore, Fig. 3b reveals the FESEM image associated with FNSCS. In the micrograph obtained from the new synthesized magnetic nanocomposite, it is well observed that the size of the particles of this nano catalyst ranged from 20 to 70 nm. Clearly, this material had bulk properties and had a tendency to convert to an accumulated form, with this agglomeration state possibly due to its magnetic properties, where the different particles or parts of the material had absorbed each other and were arranged alongside each other.

EDS or EDX is a semi quantitative method for determining the percentage of elements in a sample. This method is based on interaction between an electron analysis, EDS source and the sample. This process allows for receiving a range of elements in the sample by processing the generated X-ray. The descriptive potentials of this method are generally based on the fact that every element has a unique atomic structure (peaks). Based on Fig. 3c, the peaks shown in each diagram were associated with one of the atoms of the synthesized nanocomposite and the height of the peak represented the concentration of the element of interest in the sample, where the higher peak led to the greater percentage of the presence of the material. As can be seen in the image, the maximum weight percentage in FNSCS was associated with Cu and S, while the minimum percentage belonged to Si in the investigation of the parameters affecting photocatalytic degradation of TC.

Fig. 3d shows the VSM analysis of each of the nanoparticles $FeNi_3$ and $FeNi_3/SiO_2$ with the new nanocomposite $FeNi_3/SiO_2/CuS$, separately. The obtained magnetic resonance curves show that nanoparticles and synthesized nanocomposite have a good magnetic property, and the magnetic saturation value of $FeNi_3$, $FeNi_3/SiO_2$ and $FeNi_3/SiO_2/CuS$ is 68.52, 58.99 and 19.42, respectively. Thus, the synthesis of the final material in this study showed that FNSCS still has an acceptable magnetic property. Accordingly, it can be concluded that $FeNi_3/SiO_2/CuS$ is dispersed easily in water and can be collected by external magnetic field quickly and then can be easily dispersed with a slight twitch (Lu et al., 2016).

The XRD patterns of $FeNi_3$, $FeNi_3/SiO_2$ and $FeNi_3/SiO_2/CuS$ have been presented in Fig. 3 e_1.

Three diffraction peaks for $FeNi_3$ ($2\theta = 75.47°$, 53.56°, and 44.22°) marked by the indexes ((022), (002) and (111)), respectively, were observed. Moreover, it was found that the crystal system of $FeNi_3$ is Cubic (ICSD Collection Cod: 040,334). Furthermore, the wide peak ($2\theta = 10°–25°$) represented with code of (200) show amorphous silica (Fig. 3 e_2 (ICSD Collection Cod: 646,573). Thus the presence of silica layer in the catalyzer is confirmed (Nasseri and Sadeghzadeh, 2013). 2θ regions equal to 29.35°, 31.85°, 33.00°, 39.06°, 49.04° and 59.38° identified by index ((201), (301), (600), (501), (701) and (611)), respectively are the peaks in relation to CuS (ICSD Collection Cod: 032,105) (Fig. 3e_3). The size of the synthesized nanoparticles and the most intense diffraction peak was calculated by the Debye-Sherrer equation Eq. (1) as 48 nm, considering the full width at half maximum (FWHM). Nevertheless, it has been reported that particles size determined by TEM and SEM methods are sometimes larger than sizes determined by XRD methods. This difference could be attributed to two reasons:

1) In SEM and TEM, the obtained nanoparticles tend to accumulate due to magnetic properties, and thus the particles size was larger than the size obtained from the Debye-Sherrer equation which is sometimes higher or lower than 70 nm.
2) TEM and SEM methods showed the particle size while the XRD methods determined the crystalline size; knowing that the crystalline size is usually smaller than the particle size (Suryanarayana, 2004).

3.3. TC adsorption experiments

The experiments of absorption of tetracycline by $FeNi_3/SiO_2/CuS$ magnetic nanocomposite in conditions with pH (3, 5, 7 and 9), dose of nanocomposite (0.005–0.1 g L^{-1}), initial concentrations of TC (30-10 mg L^{-1}), contact time (5–180 min) and temperature (5–50 °C) were performed in the batch system. The effect of pH in the TC absorption process was investigated in 200 ml samples at a concentration of 20 mg L^{-1} and absorbent dose of 0.02 g L^{-1} at room temperature (24 ± 2 °C) at different pHs. The results are presented in Fig. 4 b. As can be seen, the absorption of tetracycline at a contact time of 60 min at pH 3, 7, and 9 is 52.24, 37.74 and 25.24%, respectively. This decrease can be attributed to the electrical charges of TC as well as the superficial charge of the absorbent in different pH_s. When the pH is in acidic environment, the absorbing surface is bombarded with H^+ ions. So this type of surface is very suitable for adsorption of negative charge ions. In addition, tetracycline is present in acidic, neutral and alkaline environments with functional groups such as amine, carboxylic, phenolic, alkylic and ketone. According to Fig. 1 and Table 1, tetracycline has 3 types of acid decomposition (PK_a) (3.3, 7.7 and 9.7). In acidic conditions, due to proton bombardment of dimethylamine groups in tetracycline, this pollutant has a positive charge and has positive/negative loads at pH values of 3.7–7.7 in neutral form. This kind of tetracycline molecule in neutral conditions is due to the fact that the amount of protons in the semi-saturated group of phenotype diketone has been lost. Finally, tetracycline molecules have a negative charge in alkaline

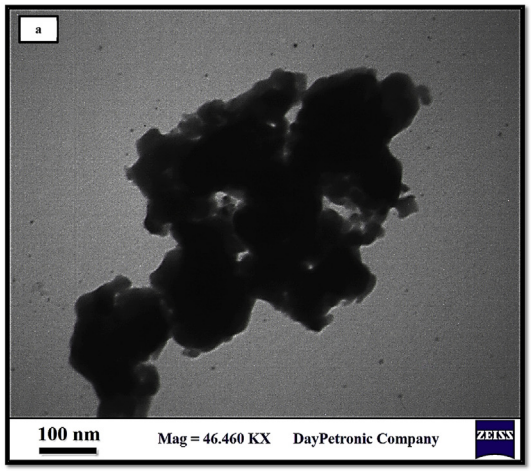

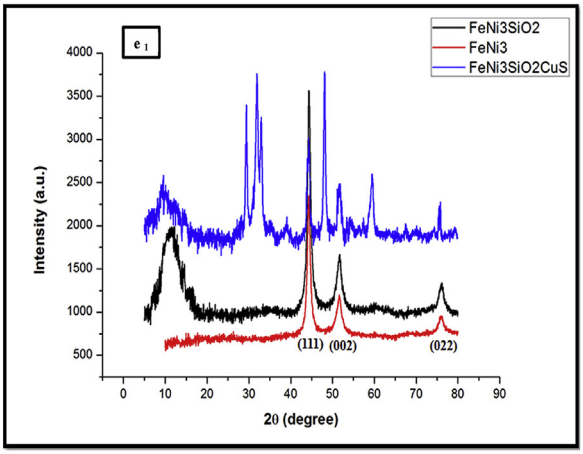

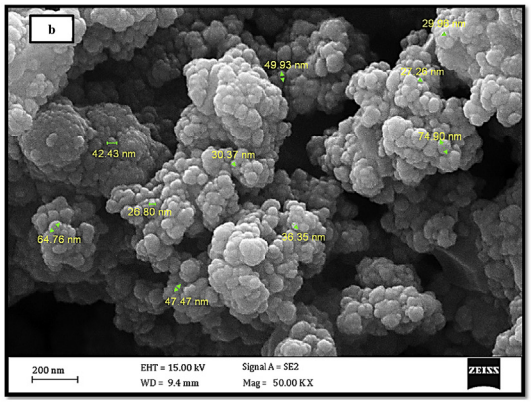

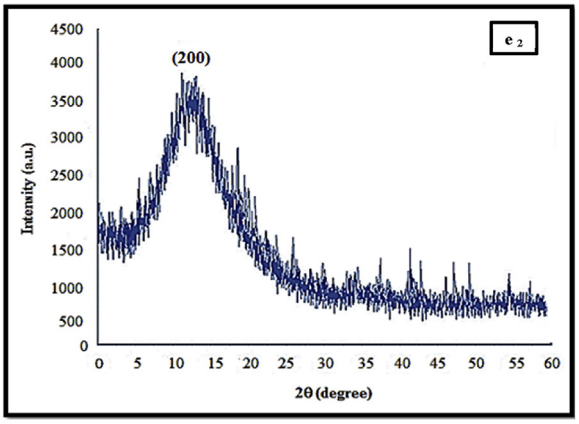

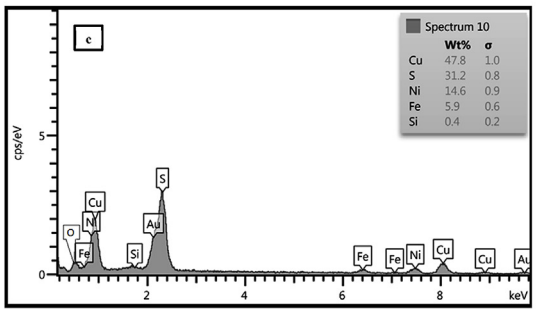

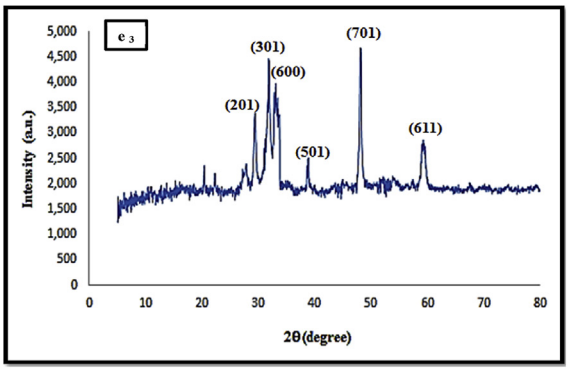

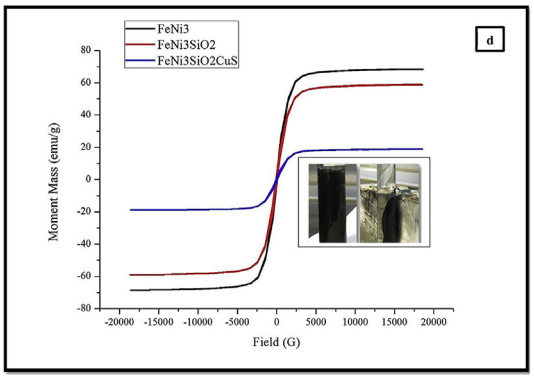

Fig. 3. The morphology and other characteristics of the magnetic nanocomposites.

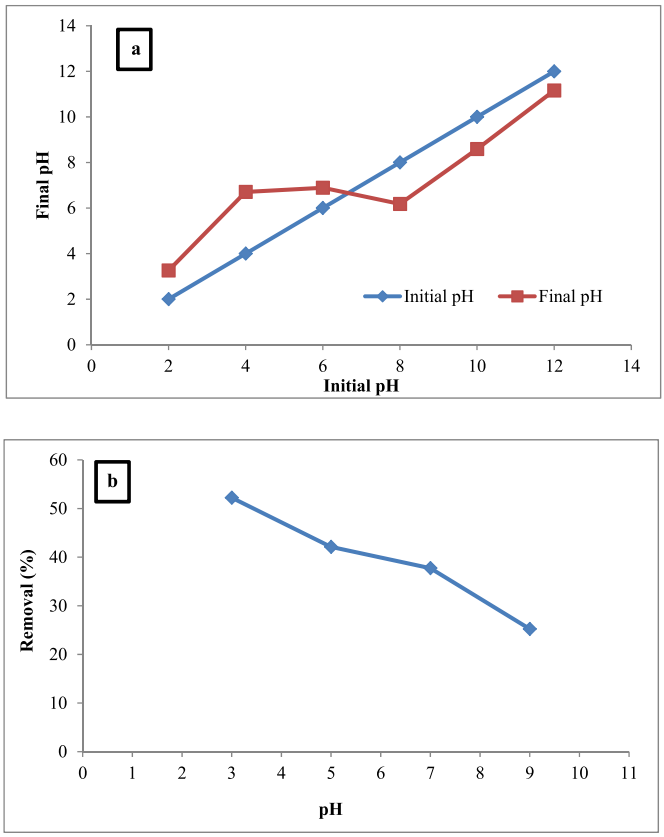

Fig. 4. Tetracycline absorption experiments on the $FeNi_3/SiO_2/CuS$ nanocomposite. a) Zeta potential of $FeNi_3/SiO_2/CuS$ at different pH values, b) Tetracycline (TC) adsorption by nanocomposite $FeNi_3/SiO_2/CuS$ with different pH (initial TC concentration = 20.0 mg L^{-1}, FNSCS dose = 0.02 g L^{-1}, Time: 200 min).

environments (Gómez-Pacheco et al., 2012; Chen and Huang, 2010). Besides, the absorber isoelectric point (pH_{zpc}) is about 6.25 (Fig. 4 a), as it is well known, the charge level of the absorbent in $pH < pH_{ZPC}$ is positive and at a pH higher than pH_{ZPC}, the adsorbent has a negative charge. According to the above description, the effect of the pH of the solution on the efficiency of tetracycline removal can be justified by the $FeNi_3/SiO_2/CuS$ adsorbent. In acidic pH less than 5.5, most of the predominant species in tetracycline have a negative and somewhat positive load, while the adsorbent surface has a positive charge. Therefore, electrostatic gravity between negative tetracycline molecules and adsorbent positive surface will increase the absorption efficiency (Noorisepehr et al., 2014). Following this, with increase in the pH of the solution and reaching about 9, the adsorbent level has a negative charge due to the presence of negative charge ions (OH^-), and on the other hand, tetracycline molecules also have a negative charge. Therefore, the efficiency of the absorption process is reduced.

Furthermore, at 180 min, the efficiency of TC adsorption increased from 37.02 to 69.02% by increasing $FeNi_3/SiO_2/CuS$ nanocomposite dosage. This can be due to the enhancement in exchange sites at the adsorbent surface. In addition, absorption percentage decreased (from 79.92 to 53.02%) with the elevation of the initial concentration of TC (from 10 to 30 mg L^{-1}) at 180 min, which was due to the fact that FNSCS absorbent has a limited number of active sites, which might be saturated at high concentrations (Ali et al., 2018; Nasseh et al., 2017b). Eventually, in the adsorption process, it was found that with the elevation of temperature from 5 to 20 °C, there was a remarkable increase in the removal percentage of TC (from 41.3 to 68.02%), while the temperature increased from 20 to 50 °C, the extent of pollutant adsorption grew mildly (68.02–73.84%) at 180 min. The reason for the elevated removal percentage, in this part can be attributed to the increase in adsorption reaction rate, because the adsorption process is endothermic (Nasseh et al., 2017a).

3.4. Investigation of the parameters affecting photocatalytic degradation of TC

3.4.1. The effect of pH

Based on the results obtained from various studies, pH plays an important role in the degradation and removal of antibiotics. In advanced oxidation processes, pH can have a huge influence on absorption capacity, distribution of electric charge on the catalyst surface, degradation rate of the contaminant, and oxidation potential of the valence band. In this research, pH also had a significant effect on the process of degradation of TC, so that at pH = 9 and pH = 3, the highest and lowest degradation percentage, respectively, were obtained (Fig. 5a). Accordingly, photocatalytic degradation of TC better occurred in alkaline conditions (Gómez-Pacheco et al., 2012).

Previous studies have explained this based on the fact that with elevation of pH of the solution, quantum efficiency of TC increased. TC is an amphoteric molecule with multiple ionizing functional groups. As mentioned earlier, different functional groups of TC had different pK_a at various pHs in aqueous environments. According to Fig. 1, three protonated functional groups were introduced in TC molecule including TC_1 (tricarbonyle methane group), TC_2 (phenolic deketone group), and TC_3 (dimethyl amino group) as presented in Fig. 1. Therefore, the effect of changes of pH on degradation rate and quantum efficiency of TC can be attributed to dominance of one or several genera of TC in environments with different pHs. Various research projects have also reported the same results (Pablos et al., 2010). This study showed that in a photocatalytic process, where there was H_4TC^+ in the environment, TC degradation was minimum. At pH = 3, after 200 min, the contaminant removal percentage reached 75.6%, whereas when H_2TC^- was dominant, the removal percentage in this process increased (in pH = 9, reaching 99.5% within this time), since electron density in the cyclic system of H_2TC^- was larger than that in H_4TC^+ in TC molecule, and thereby enhanced the aggression of radical genera (Pablos et al., 2010; Xue et al., 2015). This is in line with the results obtained by Xue Zheua et al. Yan Ma et al. (Xue et al., 2015; Ma et al., 2012).

Also, according to the semiconductive photocatalytic processes mechanism, the most important agents of oxidation at neutral and alkaline pHs were OH radicals, which resulted from the reaction between hydroxide ions (OH^-) and positive holes (Long et al., 2017). On the other hand, at acidic pHs, the most important oxidizing agents were on the positive holes (Safari et al., 2015). Furthermore, the surface available to the magnetic nanocomposite for absorbing TC and optical photons decreased at acidic pH in aqueous solutions, as the nanocatalyst particles intended to accumulate and agglomerate, and thus the removal percentage of this process was lower at acidic pHs. The reaction mechanism can be listed as follows (Xue et al., 2015):

$$Photocatalyst \xrightarrow{h\vartheta} h^+ + e^- \quad (7)$$

$$H_2O + h^+ \rightarrow \bullet OH + H^+ \quad (8)$$

$$OH^- + h^+ \rightarrow \bullet OH \quad (9)$$

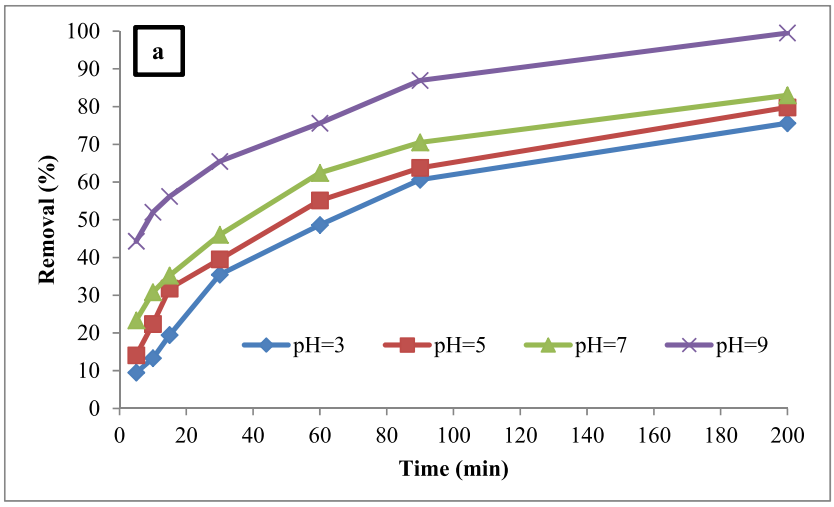

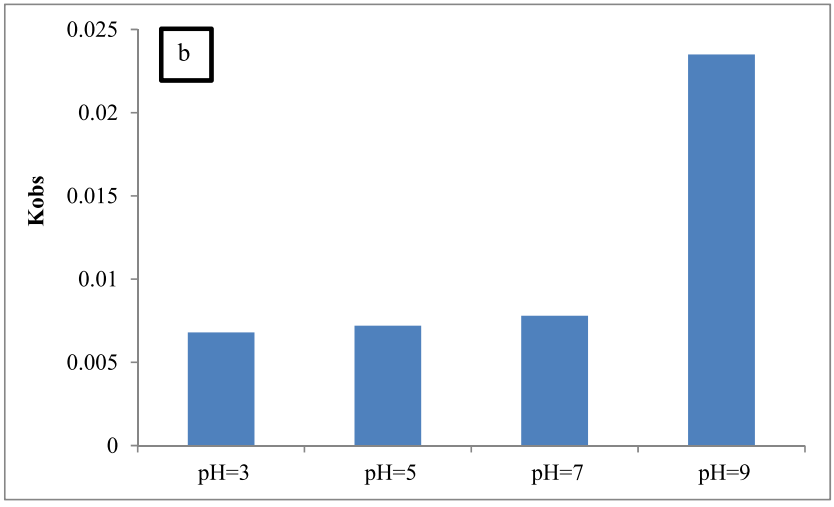

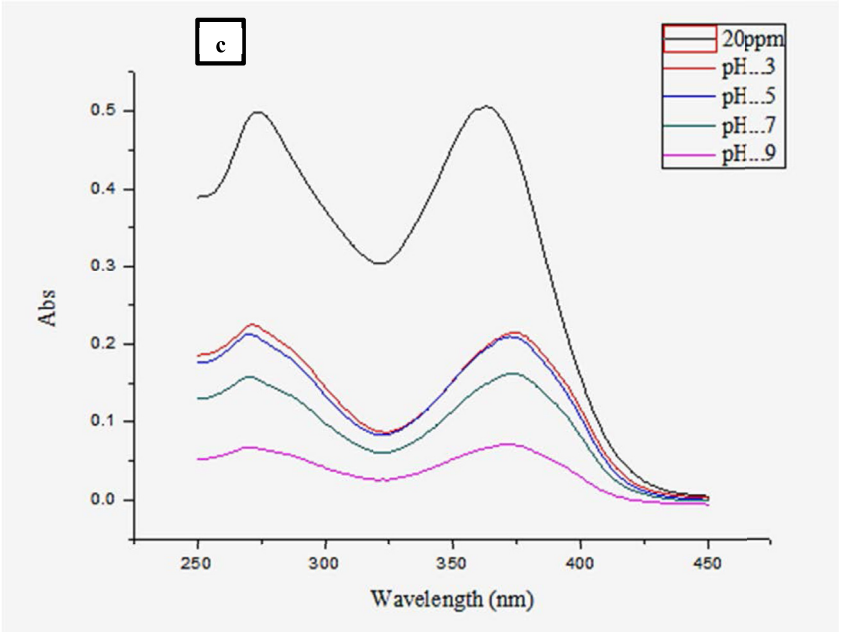

Fig. 5. a) Tetracycline (TC) degradation by nano photocatalysis $FeNi_3/SiO_2/CuS$ with different pH. b) Compare of the reaction rate constant (k_{obs}) for photocatalytic degradation of TC at different pH.

$$O_2 + e^- \rightarrow \bullet O_2^- \quad (10)$$

$$\bullet O_2^- + H^+ \rightarrow \bullet HO_2 \ (PK_a = 4.88) \quad (11)$$

$$\bullet HO_2 + \bullet HO_2 \rightarrow H_2O_2 + O_2 \quad (12)$$

$$\bullet O_2^- + \bullet H_2 \rightarrow HO_2^- + O_2 \quad (13)$$

$$HO_2^- + H^+ \rightarrow H_2O_2 \quad (14)$$

According to Equations (7)–(9), it is understood that the formation of the •OH under UV light causes reaction positive holes and H_2O as well as OH^- on the surface of photocatalyst.

If in the acidic condition of the solution, H^+ ions are too high and concentration of OH^- ions is low, the production of •OH is stopped. In addition, the reaction of Equation (11) was done in the opposite way. Therefore, the generation of $\bullet OH_2$ is reduced. As a result of this change, the reaction in Equations (12)–(14) is stopped and finally these reactions led to inhibition of oxidation. Based on these changes, photocatalytic processes do much better in neutral or alkaline condition rather than acidic condition.

The results of changes in pH indicated that the kinetics of the photocatalytic reaction of FNSCS in removing TC followed the PFO model with a correlation coefficient of $R^2 > 0.9$. Furthermore, K_{obs} at pHs 3 and 9 was obtained as 0.0068 and 0.235 min^{-1}, respectively, suggesting high reaction rate at pH = 9. Fig. 5b represents K_{obs} across different pHs of this process. Furthermore, Fig. 5c demonstrates the absorption spectrum associated with photocatalytic degradation of TC across different pHs. As can be observed, the highest peak was related to initial concentration of TC (20 mg L^{-1}). The other spectra were associated with the removal of TC across different pHs. Based on the image, it is evident that at different pHs, the absorption spectrum of the contaminant was higher and with elevation of pH toward neutral and especially alkaline pHs, the height of the peak declined, confirming the increased removal percentage of TC at pH = 9.

3.5. Comparison of UV–Visible spectra of TC in different pH

3.5.1. The effect of the dose of FNSCS

The effect of the dose of FNSCS was examined within the range of 0.005–0.01 g L^{-1} in the presence of UV light for degradation of TC. The experiments were conducted on 20 mg L^{-1} TC at pH = 9. As can be seen in Fig. 6, the removal efficiency of TC decreased in the presence of UV light with elevation of the FNSCS dose, such that after 200 min, at 0.005 and 0.1 g L^{-1}, the removal percentage decreased to95.54 and 57.7%, respectively.

Numerous studies have confirmed these results (Lu et al., 2017a), where it seems that development of turbidity in the solution with elevation of the content of FNSCS is one of the reasons for the diminished removal efficiency of TC, causing a complete disorder in transmission of light in the solution (Eslami et al., 2016; Safari et al., 2015; Xue et al., 2015). To remove turbidity and investigate the effect of elevation of the FNSCS dose in removing the contaminant in the presence of UV light, the blending factor was removed and the nanoparticles were poured into the UV pilot without turning on the magnetic stirrer. The results showed that in spite of the increased removal percentage with elevation of the FNSCS dose (at 200 min of contact time, the removal percentage grew from 33 to 49.6% for 0.005 and 0.1 g L^{-1}, respectively), it was insignificant in comparison with the time when blending occurred in the pilot; this is because the maximum removal percentage of the contaminant in the photocatalytic process with the blending was 96.17%, which was significantly different from the rate obtained during the absence of blending. This result confirms that blending in the pilot is a very important determining factor for contaminant removal (Fig. 7).

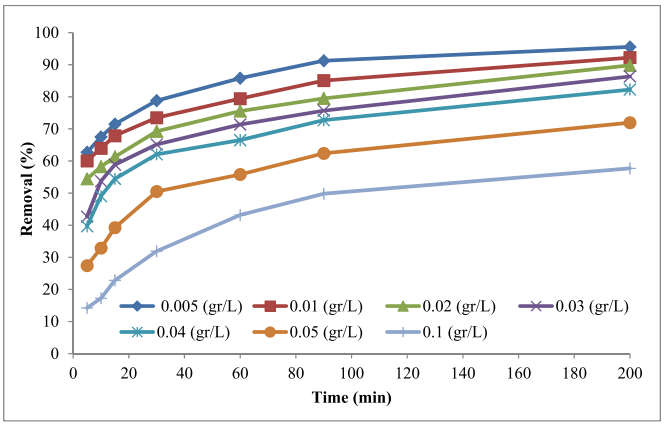

Fig. 6. Effect of Nanocomposite Dosage in the presence of UV light on tetracycline degradation.

The second reason for the diminished removal percentage with elevation of the nano catalyst dose can be attributed to the fact that at high doses, the nanocomposite finds an agglomerated or precipitated form, causing diminished active sites available for absorption of photons on its surface (Rashid et al., 2015).

As can be seen in Fig. 6, the removal efficiency occurred with a high rate at early minutes, such that at 90 min, the removal percentage increased significantly, after which the TC removal percentage in this photocatalytic process did not have a considerable increase and the rate of contaminant degradation did not increase significantly. Therefore, the optimal nanocomposite dose and irradiation time for the FNSCS/UV process were 0.005 g and 90 min, respectively, which is also very economical. It is probable that in real wastewaters, due to the presence of different anions including bromine, phosphate, chlorine, and sulfate, diminished permeation of light would occur in the photocatalytic process, thereby decreasing the removal percentage. The above results are in line with the results of other studies reported on photo catalysis of 2-chlorophenol (Rashid et al., 2015), TC (Xue et al., 2015; Safari et al., 2015), amoxicillin, ampicillin, and cloxacidine (Elmolla and Chaudhuri, 2010).

Furthermore, Eslami et al. in their study used a photocatalytic

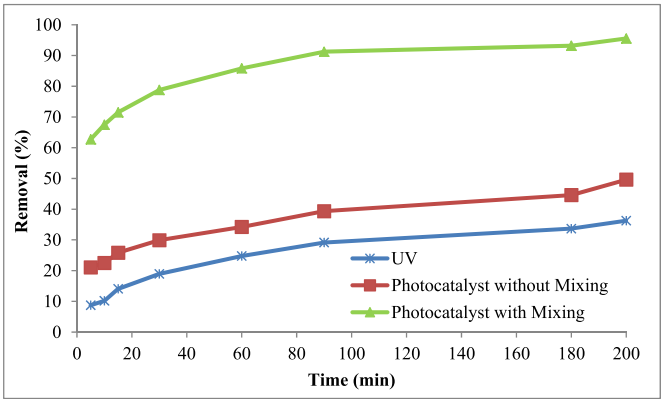

Fig. 7. Compare of tetracycline degradation in various processes with optimal conditions.

degradation process of nonsteroidal anti-inflammatory drugs of naproxen and ibuprofen and N, S co-doped TiO_2 nanoparticles in the presence of visible light. They found that the extent of degradation of these drugs increased with elevation of the nanocomposite dose from 0.5 to 2 g L^{-1}. However, further elevation above 2 g L^{-1} resulted in diminished efficiency of the process (Eslami et al., 2016). Similarly, regarding photocatalytic degradation of TC using TiO_2 nanoparticles in the presence of UV light, Safari et al. conducted a study and found that the maximum extent of degradation occurred at 1 g L^{-1} of TiO_2 (Safari et al., 2015).

3.5.2. The effect of tetracycline (TC) concentration and contact time

To examine the effect of TC concentration on the removal efficiency, different concentrations of TC (10, 15, 20, 25, and 30 mg L^{-1}) were used across seven different contact times with the optimized concentration of FNSCS (0.005 g L^{-1}) at pH = 9. The results are provided in Fig. 8. As can be seen, the TC removal percentage decreased significantly with elevation of the concentration. For instance, the TC removal efficiency at 10 mg L^{-1} at 90 min was obtained as 96.71%, whereas this efficiency at the initial concentrations of 15, 20, 25, and 30 mg L^{-1} was 90.39, 84.34, 81.4, and 78.23%, respectively. The reason for the elevation of photocatalytic degradation with reduction of the TC concentration can be attributed to the fact that under similar conditions, the FNSCS concentration, contact time, and pH of the density of hydroxyl (•OH) free radicals were equal in the solution. Accordingly, TC reaction with •OH grew at lower concentrations, causing increased degradation of TC by free radicals. In addition, with elevation of the concentration of the contaminant, the ray radiated by TC molecules was absorbed and did not reach the surface of all catalyst particles. Moreover, in response to lack of excitement of all the catalyst particles, the extent of degradation decreased significantly (Safari et al., 2015).

Note that UV radiation alone was effective in removing TC by 33.26% within 200 min.

To investigate the kinetics of photocatalytic degradation of TC in the FNSCS/UV process across different concentrations, the experiments were conducted under optimal conditions (nanocatalyst dose: 0.005 g L^{-1}, contact time: 90 min, and pH = 9). The initial concentration of TC for investigation of the TC degradation kinetics and optical process mechanism was determined after 30 min of absorption and darkness (Safari et al., 2015). The results revealed that the (PFO) kinetics model was a suitable model for describing the rate of this reaction and covered the results for all different concentrations of TC, such that R^2 values were close to 1 and the reaction rate constant diminished with elevation of the TC concentration (Dimitrakopoulou et al., 2012). At high concentrations, due to elevation of the concentration of transition products, the activated hydroxyl radicals in the reaction became limited and therefore decreased the degradation rate constant (Fig. 9 and Table 2).

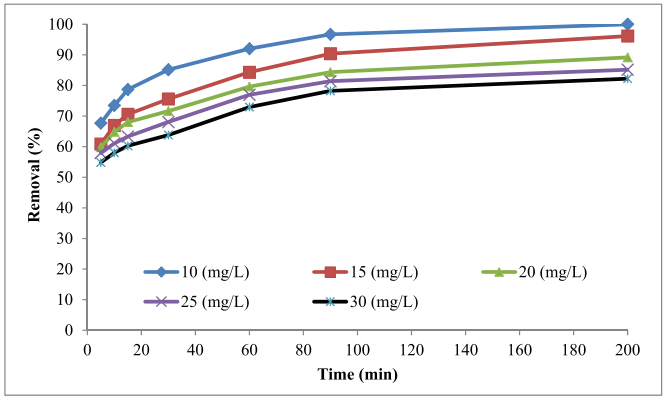

Fig. 8. Effect of initial concentration of tetracycline in the presence of UV light.

Based on the results obtained from the previous steps for optimizing the parameters affecting the photocatalytic degradation of tetracycline, the mineralization rate of this process in optimal conditions (tetracycline concentration: 20 mg L^{-1}, time: 200 min, pH = 9, nanocatalyst dose: 0.005 g L^{-1}) was obtained by the ANA TOC device made by SGE Australia, using the method of 5310 B, the Standard Methods - For the examination of water and wastewater(Federation and Association, 2005).

The results showed that the initial TOC of tetracycline before the start of the degradation process was 117 but after the completion of the process, reached 41. In other words, the mineralization rate of this process was 64.96%.

3.6. Experiment for investigation of stability and recycle of $FeNi_3/SiO_2/CuS$

A key parameter for measuring the activity and stability of solid catalysts can be their recycling. For this purpose, to investigate the recoverability or recyclability of the nanocomposites synthesized in this research as an optical catalyst, TC degradation experiments were conducted in 5 periodic cycles under the following conditions: TC concentration = 20 mg L^{-1}, FNSCS/UV dose = 0.01 g L^{-1}, contact time = 90 min, and pH = 9. Following each cycle, the nano catalyst of interest was separated from the solution by a magnet, washed several times with deionized water, dried in an oven at 80 °C, and reused in the beginning of the next cycle of TC removal. Eventually, the residual concentration of TC following each individual cycle was measured.

The results of the experiments are provided in Fig. 10, suggesting that following the five cycles, the nano catalyst efficiency did

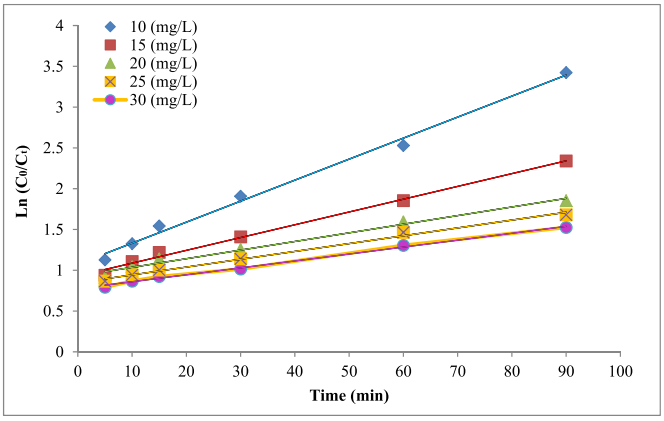

Fig. 9. The kinetic curve of the pseudo-first-order equation of tetracycline degradation at different concentrations.

Table 2
Kinetics parameters of pseudo-first-order for degradation of TC degradation at different concentrations.

Concentration (mg/L)	Equation	K_0 (min^{-1})	R^2	$t_{1/2}$ (min)
10	Y = 0.0257x+1.0758	25.7×10^{-3}	0.9933	26.9
15	Y = 0.0157x+0.9309	15.7×10^{-3}	0.9938	44.1
20	Y = 0.0106x+0.9305	10.6×10^{-3}	0.9849	65.37
25	Y = 0.0096x+0.8483	9.6×10^{-3}	0.9849	72.2
30	Y = 0.0085x+0.7747	8.5×10^{-3}	0.9952	81.53

$t_{1/2} = 0.693/K_0$.

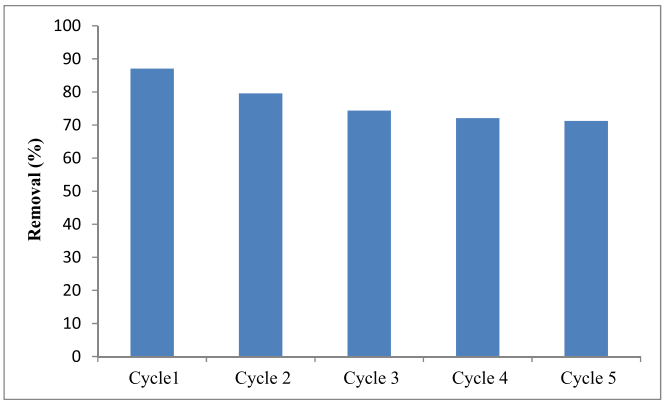

Fig. 10. Diagram of tetracycline antibiotic degradation in photocatalytic process of $FeNi_3/SiO_2$/Cus nanocomposite in during 5 cycles of reuse.

not have a significant reduction; accordingly, the removal efficiency was 87.07% in the first cycle, which decreased to 71.24% in the last cycle, showing only 15.83% reduction. This can be due to the diminished mass of the nano composition over the several cycles (Kakavandi et al., 2016; Zhang et al., 2015). Based on this stage of the experiment, it can be concluded that this synthesized nanocomposite is not deactivated along the optical catalytic reactions and its application is economical in terms of operational costs due to its high reusability potential.

3.7. CuS photocatalysis mechanism

The main characteristics of semiconductor photocatalytic process are Valence and Conduction bands. The area between these two bands is called “Band Gap".

When optical photons of equal or higher energy ($h\upsilon$) than the band gap of CuS photocatalysis illuminates the semiconductor, the photo excitement of the Valence band electron as well as the absorption of radiation occurs. Therefore, the excited electrons (e^-) existing in the Valence band are transmitted to the conduction band. This results in the promotion of positive hole (h^+) in the valence band (Equation (15)).

$$CuS \xrightarrow{h\vartheta} CuS\left(e^- + h^+\right) \quad (15)$$

The $e^-$and h^+ can both move to the surface of the CuS catalyst, in which they can begin remediation reactions with other species.

The positive holes (h^+) are excellent oxidants that can result in direct and indirect oxidation of adsorbent pollution (TC). When the oxidation process is direct, the pollutants are oxidized by h^+ (Equation (16)).

$$\left(h^+\right) + TC \rightarrow TC^+ \quad (16)$$

Besides, when the oxidation process is indirect, the h^+ can react with electron donors such as hydroxyl ions and water in order to produce strong oxidizing •OH radicals (Equations (17) and (18)).

$$\left(h^+\right) + H_2O \rightarrow \bullet OH + H^+ \quad (17)$$

$$\left(h^+\right) + OH^- \rightarrow \bullet OH \quad (18)$$

In the case e^-, electron acceptors can scavenge them to stop the recombination with h^+.

The molecules of oxygen (O_2) are among the acceptors which can be reduced by the e^- to superoxide form ($\bullet O_2^-$) (Equation (19)).

$$e^- + O_2 \rightarrow \bullet O_2^- \quad (19)$$

Therefore, a series of more reactions could occur to generate an additional pathway of radical OH (Equations (20)–(24)).

$$\bullet O_2^- + H^+ \rightarrow \bullet HO_2 \quad (20)$$

$$2 \bullet HO_2 \rightarrow H_2O_2 + O_2 \quad (21)$$

$$H_2O_2 + \bullet O_2^- \rightarrow OH^- + \bullet OH + O_2 \quad (22)$$

$$H_2O_2 + e^- \rightarrow OH^- + \bullet OH \quad (23)$$

$$H_2O_2 + \left(h^+\right) \rightarrow 2 \bullet OH \quad (24)$$

These active radicals can degrade TC.

$$TC + (\bullet OH, \bullet HO_2, \bullet O_2^- \text{ or } (h^+) \rightarrow intermediates \rightarrow final\ products \quad (25)$$

We can see from the above mechanism that electron-hole pair is very important in the reaction of photocatalysis (Lu et al., 2015; Lam, 2016).

4. Conclusions

In this research, $FeNi_3/SiO_2$/CuS synthesized and characterized as a new magnetic photocatalysis for determining optimal conditions of degradation of TC was examined. Based on the analyses of the characterization of the nanocomposite, it was found that this magnetic nanocatalyst was homogeneous and synthesized properly. In addition, the results showed that FNSCS was superparamagnetic at room temperature ($Ms = 19.42$ emu g^{-1}); therefore, it can be easily separated from the solution with an external magnetic field.

This study indicated that photolysis process (in the presence of UV alone) cannot be very effective for TC removal. However, addition of the nanocatalyst synthesized in this study for this process enhances the contaminant removal percentage significantly. Accordingly, this combined process can be employed as a suitable method for removing this barely biodegradable contaminant from water and wastewater. Also, results showed that, the maximum extent of TC degradation in the presence of FNSCS and UV light reached 96.71% and the mineralization rate was 64.96%, under the optimal conditions of the reaction (contact time: 90 min, catalyst dose: 0.005 g L^{-1}, pH = 9). The kinetics of the TC photocatalytic degradation reaction followed the pseudo-first order equation ($R^2 > 0.98$) and the rate constant was obtained as 0.0257 min^{-1}.

This process was influenced by pH and the degradation rate decreased with elevation of pH from 3 to 9. With elevation of the nano catalyst dose from 0.005 to 0.01 g L^{-1}, the removal percentage decreased due to interference in UV light absorption. Furthermore, removal of TC using the intended magnetic nano catalyst diminished with elevation of the initial concentration of the contaminant. The results obtained from optical catalyst experiments indicated that the new nanocomposite synthesized in this research enjoyed a high recoverability and reusability, as the TC removal percentage diminished by only 15% following five periodic cycles, since the descending trend of the removal percentage was lower in the final cycles, when compared with the early cycles. Eventually, based on the results obtained in this research, it can be concluded that the FNSCS photocatalytic process enjoys a suitable efficiency for removing TC from aqueous environments and it is economical regarding its recyclability.

Acknowledgments:

This paper is derived from a PhD thesis on environmental pollution approved by the Natural resources and Environment faculty, the Islamic Azad University, Science and Research Branch. The authors of this paper acknowledge the Vice Chancellor for Research at this university and the health faculty at the Birjand University of Medical Sciences for their never-ending support.

References

Ali, M.M., Ahmed, M., Hameed, B., 2018. NaY zeolite from wheat (Triticum aestivum L.) straw ash used for the adsorption of tetracycline. J. Clean. Prod. 172, 602–608.

Almasi, A., Dargahi, A., Mohamadi, M., BiglariI, H., Amirian, F., Raei, M., 2016. Removal of Penicillin G by combination of sonolysis and Photocatalytic (sono-photocatalytic) process from aqueous solution: process optimization using RSM (Response Surface Methodology). Electron. Physician 8, 2878.

Amouzgar, P., Salamatinia, B., 2015. A short review on presence of pharmaceuticals in water bodies and the potential of chitosan and chitosan derivatives for elimination of pharmaceuticals. J. Mol. Genet. Med. S 4, 1747–10862.

Assadi, A., Dehghani, M.H., Rastkari, N., Nasseri, S., Mahvi, A.H., 2012. Photocatalytic reduction of hexavalent chromium in aqueous solutions with zinc oxide nanoparticles and hydrogen peroxide. Environ. Protect. Eng. 38, 5–16.

Barhoumi, N., Otran, N., Ammae, S., Gadri, A., Oturan, M.A., Brillas, E., 2017. Enhanced degradation of the antibiotic tetracycline by heterogeneous electro-Fenton with pyrite catalysis. Environ. Chem. Lett. 15, 689–693.

Beyki, M.H., Shirkhodaie, M., Shemirani, F., 2016. Polyol route synthesis of a Fe_3O_4@CuS nanohybrid for fast preconcentration of gold ions. Anal. Math. 8, 1351–1358.

Caroni, A., De Lima, C., Pereira, M., Fonseca, J., 2009. The kinetics of adsorption of tetracycline on chitosan particles. J. Colloid Interface Sci. 340, 182–191.

Chen, W.-R., Huang, C.-H., 2010. Adsorption and transformation of tetracycline antibiotics with aluminum oxide. Chemosphere 79, 779–785.

Daghrir, R., Drogui, P., 2013. Tetracycline antibiotics in the environment: a review. Environ. Chem. Lett. 11, 209–227.

Dimitrakopoulou, D., Rethemiotaki, I., Frontistis, Z., Xekoukoulotakis, N.P., Venieri, D., Mantzavinos, D., 2012. Degradation, mineralization and antibiotic inactivation of amoxicillin by UV-A/TiO_2 photocatalysis. J. Environ. Manag. 98, 168–174.

Elmolla, E.S., Chaudhuri, M., 2010. Photocatalytic degradation of amoxicillin, ampicillin and cloxacillin antibiotics in aqueous solution using UV/TiO_2 and UV/H_2O_2/TiO_2 photocatalysis. Desalination 252, 46–52.

Eslami, A., Amini, M.M., Yazdanbakhsh, A.R., Mohseni-bandpei, A., Safari, A.A., Asadi, A., 2016. N, S co-doped TiO_2 nanoparticles and nanosheets in simulated solar light for photocatalytic degradation of non-steroidal anti-inflammatory drugs in water: a comparative study. J. Chem. Technol. Biotechnol. 91, 2693–2704.

Federation, W.E., Association, A.P.H., 2005. Standard Methods for the Examination of Water and Wastewater. American Public Health Association (APHA), Washington, DC, USA.

Gómez-Pacheco, C., Sánchez-polo, M., Rivera- utrilia, J., López-penalver, J., 2012. Tetracycline degradation in aqueous phase by ultraviolet radiation. Chem. Eng. J. 187, 89–95.

Guo, J., Li, Y., Hu, D., Liu, H., 2014. Preparation of transition-metal-doped ZnO nanophotocatalysts and their performance on photocatalytic degradation of antibiotic wastewater. Desalination Water Treat. https://doi.org/10.1080/19443994.2014.961171.

Johar, M.A., Afzal, R.A., Alazba, A.A., Manzoor, U., 2015. Photocatalysis and bandgap engineering using ZnO nanocomposites. Advances in Materials Science and Engineering 2015. https://doi.org/10.1155/2015/934587.

Kakavandi, B., Rezaei kalantari, R., Jonidi jafari, A., Esrafily, A., Gholizadeh, A., Azari, A., 2014. Efficiency of powder activated carbon magnetized by Fe_3O_4 nanoparticles for amoxicillin removal from aqueous solutions: equilibrium and kinetic studies of adsorption process. Iran. J. Health Environ. 7, 21–34.

Kakavandi, B., Tkdastan, A., Jaafarzadeh, N., Azizi, M., Mirzaei, A., Azari, A., 2016. Application of Fe_3O_4@C catalyzing heterogeneous UV-Fenton system for tetracycline removal with a focus on optimization by a response surface method. J. Photochem. Photobiol. Chem. 314, 178–188.

Katipoglu- yazan, T., Merlin, C., Pons, M.N., Ubay-cokgor, E., Orhon, D., 2015. Chronic impact of tetracycline on nitrification kinetics and the activity of enriched nitrifying microbial culture. Water Res. 72, 227–238.

Lam, L.S., 2016. Photocatalytic Degradation of Sunset Yellow Dye Over Zinc Oxide Nanoparticles under Fluorescent Light Irradiation. UTAR.

Liu, Q., Zhong, L.B., Zhao, Q.B., Frear, C., Zheng, Y.-M., 2015. Synthesis of Fe_3O_4/polyacrylonitrile composite electrospun nanofiber mat for effective adsorption of tetracycline. ACS Appl. Mater. Inter. 7, 14573–14583.

Liu, Z., Zhu, M., Wang, Z., Wang, H., Deng, C., Li, K., 2016. Effective degradation of aqueous tetracycline using a nano-TiO_2/carbon electrocatalytic membrane. Materials 9, 364.

Long, J.J., Liu, B., Wang, G.F., Shi, W., 2017. Photocatalitic stripping of fixed Reactive Red X-3B dye from cotton with nano-TiO_2/UV system. J. Clean. Prod. 165, 788–800.

Lu, Z., Huo, P., Luo, Y., Liu, X., Wu, D., Gao, X., Li, C., Yan, Y., 2013. Performance of molecularly imprinted photocatalysts based on fly-ash cenospheres for selective photodegradation of single and ternary antibiotics solution. J. Mol. Catal. Chem. 378, 91–98.

Lu, Z., Yu, Z., Dong, J., Song, M., Liu, Y., Liu, X., Fan, D., Ma, Z., Yan, Y., Huo, P., 2017a. Construction of stable core–shell imprinted Ag-(poly-o-phenylenediamine)/$CoFe_2O_4$ photocatalyst endowed with the specific recognition capability for selective photodegradation of ciprofloxacin. RSC Adv. 7, 48894–48903.

Lu, Z., Yu, Z., Dong, J., Song, M., Liu, Y., Liu, X., Ma, Z., Su, H., Yan, Y., Huo, P., 2017b. Facile microwave synthesis of a Z-scheme imprinted $ZnFe_2O_4$/Ag/PEDOT with the specific recognition ability towards improving photocatalytic activity and selectivity for tetracycline. Chem. Eng. J. https://doi.org/10.1016/j.cej.2017.12.115.

Lu, Z., Zhao, X., Zhu, Z., Yan, Y., Shi, W., Dong, H., Ma, Z., Gao, N., Wang, Y., Huang, H., 2015. Enhanced recyclability, stability, and selectivity of CdS/C@ Fe_3O_4 nanoreactors for orientation photodegradation of ciprofloxacin. Chem. A Europe. J. 21, 18528–18533.

Lu, Z., Zhu, Z., Wang, D., Ma, Z., Shi, W., Yan, Y., Zhao, X., Dong, H., Yang, L., Hua, Z., 2016. Specific oriented recognition of a new stable ICTX@ Mfa with retrievability for selective photocatalytic degrading of ciprofloxacin. Catal. Sci. Technol. 6, 1367–1377.

Ma, Y., Gao, N., Li, C., 2012. Degradation and pathway of tetracycline hydrochloride in aqueous solution by potassium ferrate. Environ. Eng. Sci. 29, 357–362.

Ma, Y., Zhou, Q., Zhou, S., Wang, W., Jin, J., Xie, J., Li, A., Shuang, C., 2014. A bifunctional adsorbent with high surface area and cation exchange property for synergistic removal of tetracycline and Cu 2+. Chem. Eng. J. 258, 26–33.

Nasseh, N., Taghavi, L., Barikbin, B., Harifi-moodI, A.R., 2017a. The removal of Cr (VI) from aqueous solution by almond green hull waste material: kinetic and equilibrium studies. J. Water Reuse Desalination 7, 449–460.

Nasseh, N., Taghavi, L., Barikbin, B., Khodadadi, M., 2017b. Advantage of almond green hull over its resultant ash for chromium (VI) removal from aqueous solutions. Int. J. Environ. Sci. Technol. 14, 251–262.

Nasseri, M.A., Sadeghzadeh, S.M., 2013. A highly active $FeNi_3$–SiO_2 magnetic nanoparticles catalyst for the preparation of 4H-benzo [b] pyrans and Spirooxindoles under mild conditions. J. Iran. Chem. Soc. 10, 1047–1056.

Nirpuel, M., Jafari, A., Boustani, K., 2014. Magnetic and structural study of $FeNi_3$ nanoparticles: effect of calcination temperature. J. Supercond. Nov. Magnetism 27, 2803–2811.

Noorisepehr, M., Mohebi, S., Abdlollahivahed, B.,S., Zarrabi, M., 2014. Removal of tetracycline from synthetic solution by natural LECA. J. Environ. Health Eng. 1, 301–311.

Oturan, N., Wu, J., Zhang, H., Sharma, V.K., Oturan, M.A., 2013. Electrocatalytic destruction of the antibiotic tetracycline in aqueous medium by electrochemical advanced oxidation processes: effect of electrode materials. Appl. Catal. B Environ. 140, 92–97.

Pablos, J., Abrusci, C., Marin, I., López-marin, J., Catalina, F., Espí, E., Cprrales, T., 2010. Photodegradation of polyethylenes: comparative effect of Fe and Ca-stearates as pro-oxidant additives. Polym. Degrad. Stabil. 95, 2057–2064.

Papolo, M.E., Savini, M., Valles, J., Baschini, M., Avena, M., 2008. Tetracycline adsorption on montmorillonite: pH and ionic strength effects. Appl. Clay Sci. 40, 179–186.

Rashid, J., Barakat, M., Ruzmanova, Y., Chianese, A., 2015. Fe_3O_4/SiO_2/TiO_2 nanoparticles for photocatalytic degradation of 2-chlorophenol in simulated wastewater. Environ. Sci. Pollut. Control Ser. 22, 3149–3157.

Safari, G., Hoseini, M., Seyedsalehi, M., Kamani, H., Jaafari, J., Mahvi, A., 2015. Photocatalytic degradation of tetracycline using nanosized titanium dioxide in aqueous solution. Int. J. Environ. Sci. Technol. 12, 603–616.

Saitoh, T., Shibata, K., Fujimori, K., Ohtani, Y., 2017. Rapid removal of tetracycline antibiotics from water by coagulation-flotation of sodium dodecyl sulfate and poly (allylamine hydrochloride) in the presence of Al (III) ions. Separ. Purif. Technol. https://doi.org/10.1016/j.seppur.2017.06.036.

Salarian, A.A., Hami, Z., Mirzaei, N., Mohseni, S.M., Asadi, A., Bahrami, H., Vosoughi, M., Alinejad, A., Zare, M.-R., 2016. N-doped TiO_2 nanosheets for photocatalytic degradation and mineralization of diazinon under simulated solar irradiation: optimization and modeling using a response surface methodology. J. Mol. Liq. 220, 183–191.

Salvestrin, H., Hagare, P., 2009. Removal of nitrates from groundwater in remote indigenous settings in arid Central Australia. Desalination Water Treat 11, 151–156.

Saygılı, H., Guzel, F., 2016. Effective removal of tetracycline from aqueous solution using activated carbon prepared from tomato (Lycopersicon esculentum Mill.) industrial processing waste. Ecotoxicol. Environ. safety 131, 22–29.

Shekari, H., Sayadi, M., Rezaei, M., Allahresani, A., 2017. Synthesis of nickel ferrite/titanium oxide magnetic nanocomposite and its use to remove hexavalent chromium from aqueous solutions. Surfaces Interfaces 8, 199–205.

Singh, P., Priya, B., Shandilya, P., Raizada, P., SinghI, N., Pare, B., Jonnalagadda, S., 2016. Photocatalytic mineralization of antibiotics using 60% WO_3/BiOCl stacked to graphene sand composite and chitosan. Am. J. Chem. https://doi.org/10.1016/j.arabjc.2016.08.005.

Song, B., Zeng, G., Gong, J., Liang, J., Xu, P., Liu, Z., Zhang, Y., Zhang, C., Cheng, M., Liu, Y., 2017. Evaluation methods for assessing effectiveness of in situ remediation of soil and sediment contaminated with organic pollutants and heavy metals. Environ. Int. 105, 43–55.

Song, B., Zhang, C., Zeng, G., Gong, J., Chang, Y., Jiang, Y., 2016. Antibacterial properties and mechanism of graphene oxide-silver nanocomposites as bactericidal agents for water disinfection. Arch. Biochem. Biophys. 604, 167–176.

Suryanarayana, C., 2004. Mechanical Alloying And Milling Marcel Dekker, pp. 59–78. EE. UU.

Vázquez, A., Hernández- uresti, D., Obregbón, S., 2016. Electrophoretic deposition of CdS coatings and their photocatalytic activities in the degradation of tetracycline antibiotic. Appl. Surf. Sci. 386, 412–417.

Wang, M., Zhang, L., Zhang, G., Pang, T., Zhang, X., Cal, D., Wu, Z., 2017. In situ degradation of antibiotic residues in medical intravenous infusion bottles using high energy electron beam irradiation. Sci. Rep. 7, 39928.

Wang, Y., Zhang, H., Zhang, J., Lu, C., Huang, Q., Wu, J., Liu, F., 2011. Degradation of tetracycline in aqueous media by ozonation in an internal loop-lift reactor. J. Hazard Mater. 192, 35–43.

Xue, Z., Wang, T., Chen, B., Malhoske, T., Yu, S., Tang, Y., 2015. Degradation of tetracycline with $BiFeO_3$ prepared by a simple hydrothermal method. Materials 8, 6360–6378.

Yang, J., Tang, Y.F., Yan, X.S., Da, Z.L., Zhang, R.X., Huo, P.W., 2014. Synthesis of spherical CuS photocatalyst and the research on photo-degradation activity of methylene blue. Appl. Mech. Mater. Trans Tech Publ. 2014 https://doi.org/10.4028/www.scientific.net/AMM.507.716.

Yang, S.T., Zhang, W., Xie, J., Liao, R., Zhang, X., Yu, B., Wu, R., Liu, X., Li, H., Guo, Z., 2015. Fe_3O_4@SiO_2 nanoparticles as a high-performance Fenton-like catalyst in a neutral environment. RSC Adv. 5, 5458–5463.

Zhang, M., Song, W., Chen, Q., Miao, B., Hee, W., 2015. One-pot synthesis of magnetic Ni@ $Mg(OH)_2$ core–shell nanocomposites as a recyclable removal agent for heavy metals. ACS Appl. Mater. Inter. 7, 1533–1540.